# Tight Binding of Carboxylate, Phosphonate, and Carbamate Anions to Stoichiometric CdSe Nanocrystals

Peter E. Chen, Nicholas C. Anderson, Zachariah M. Norman, and Jonathan S. Owen*

*Department of Chemistry, Columbia University in the City of New York*

*New York, NY 10027.*
Email: jso2115@columbia.edu

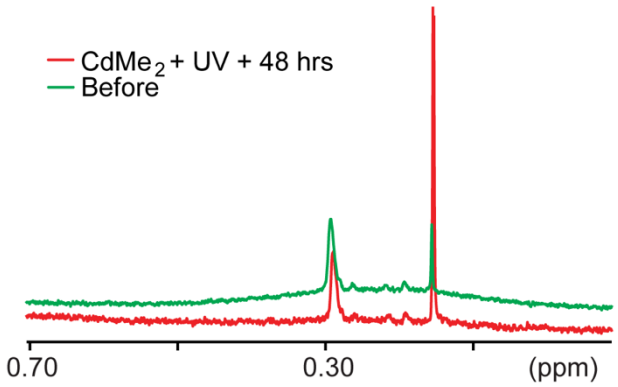


**Figure S1**. Methane region of the $^{1}$H NMR spectra of (CdSe)-Cd($O_2$CR)$_2$ treated with $CdMe_2$ that shows the decrease in bound methyl and formation of methane before (green) and after exposure (red) to UV-light. The intensities of the resonances are normalized to an internal ferrocene standard ($\delta$ = 4.0 ppm, not shown).

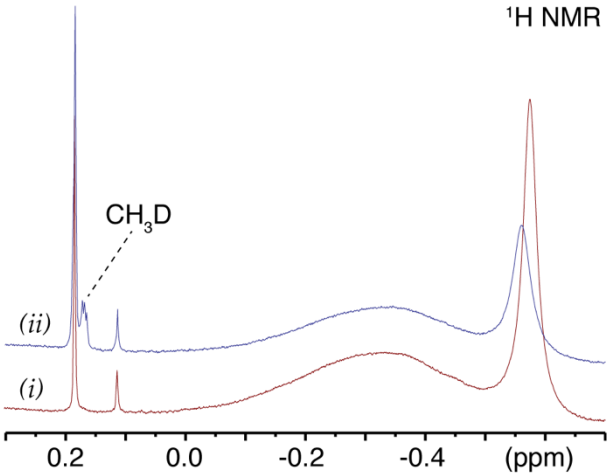


**Figure S2**. Methane region of the $^{1}$H NMR spectra of CdSe-Cd($O_2$CR)$_2$ treated with $CdMe_2$ in a solution of THF-$d_8$ (0.14 methyls per nm$^{-2}$, *i*) that shows the formation of $CH_3D$ upon exposure to UV-light (*ii*). Both a decrease in the amount of methyl species (broad resonance from -0.1 to -0.5 ppm) and an increase in the amount of $CH_3D$ (1:1:1 triplet centered at 0.17 ppm) are seen upon light exposure. The intensities of the resonances are normalized to an internal ferrocene standard ($\delta$ = 4.0 ppm, not shown).

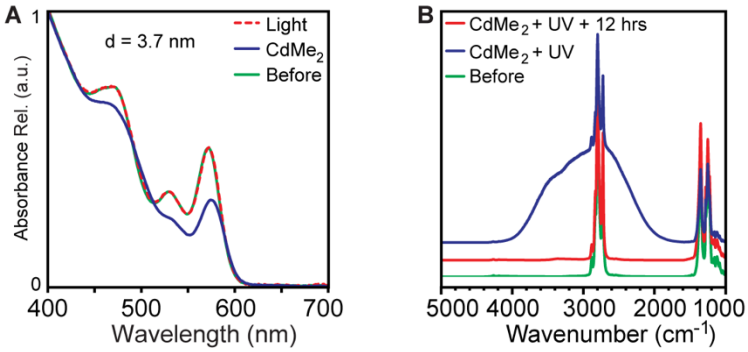


**Figure S3.** (A) UV-Vis spectra and (B) FT-IR spectra of CdSe-Cd($O_2CR$)$_2$ before (green) and after (blue) the addition of $CdMe_2$, and after exposure of $CdMe_2$ treated CdSe-Cd($O_2CR$)$_2$ with UV-light for 12 hours (red). Upon treatment with $CdMe_2$, bleaching of the first electronic transition and broadening of higher order transitions can be seen in the UV-Vis absorption spectrum. In the IR region, the appearance of a broad transition centered around 2800 $cm^{-1}$ follows brief exposure to UV-light, and then gradually dissipates over 12 hours with continued irradiation.

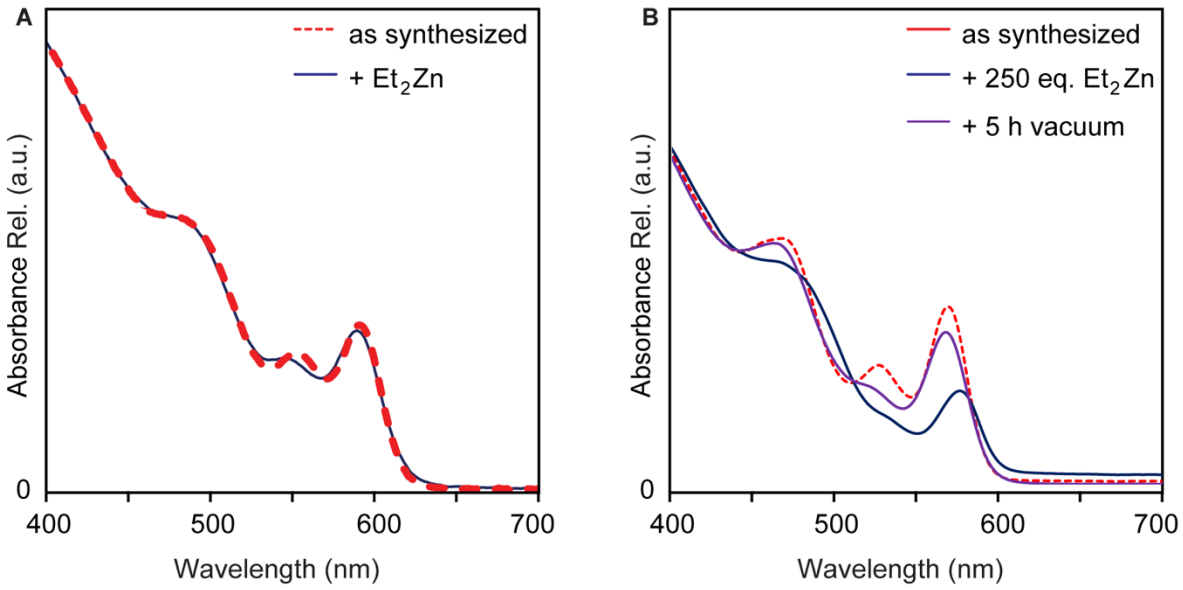


**Figure S4**. (A) UV-Vis spectra of CdSe-Cd($O_2CR$)$_2$ before (dotted, red) and after (solid, blue) treatment with diethylzinc and subsequent purification by precipitation. (B) UV-Vis spectra of a different CdSe-Cd($O_2CR$)$_2$ sample before (dotted, red), after the addition of 250 equivalents (per nanocrystal) of diethylzinc (solid, blue), and after exposure to vacuum for 5 hours (solid, purple).

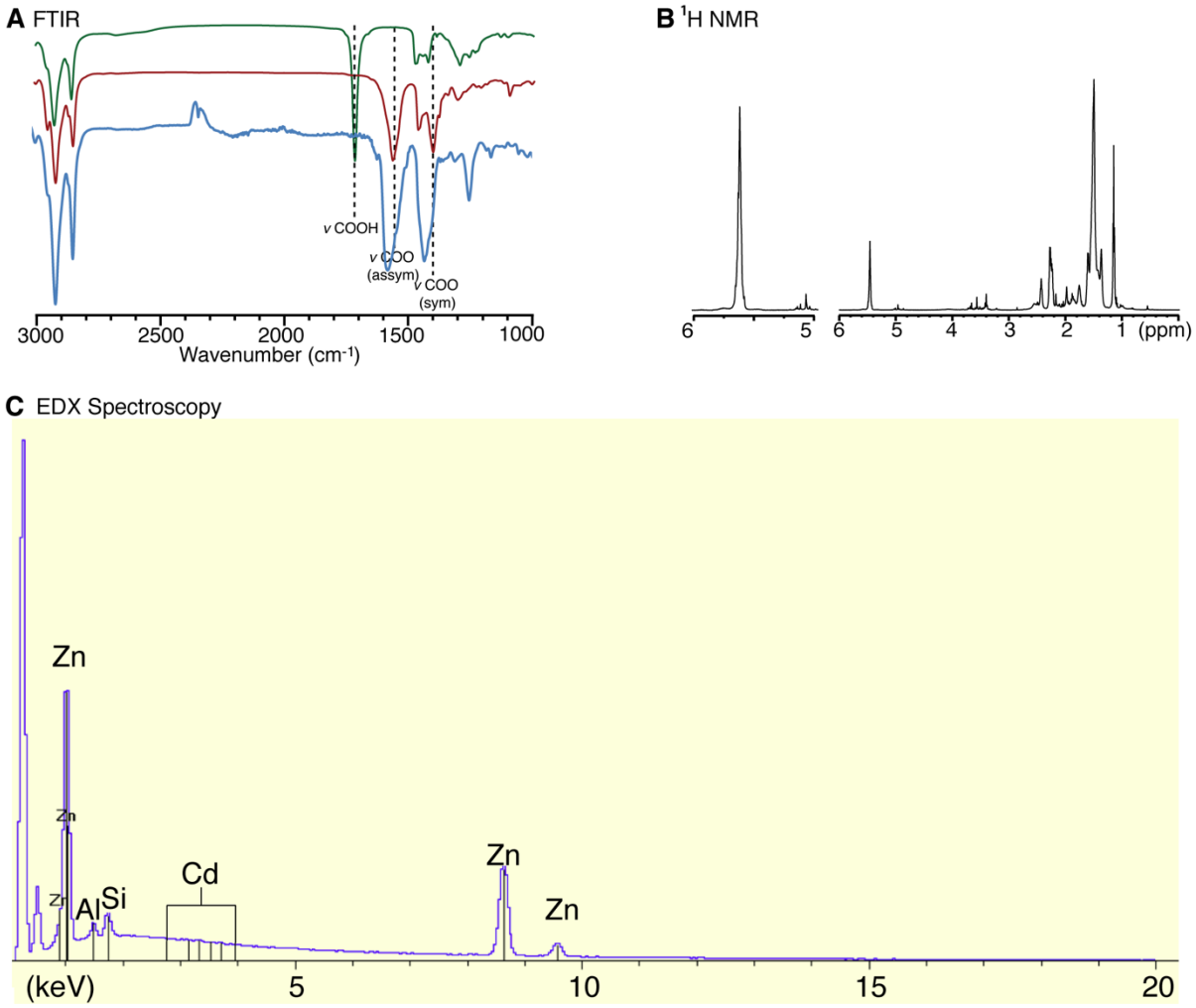


**Figure S5**. (A) FT-IR, of $Zn(O_2CR)_2$ isolated from a CdSe-$Cd(O_2CR)_2$ solution treated with diethyl zinc (blue), independently prepared zinc oleate (red), and oleic acid (green). (B) $^1H$ NMR, and (C) EDX spectra of $Zn(O_2CR)_2$ isolated from a CdSe-$Cd(O_2CR)_2$ solution treated with diethylzinc.

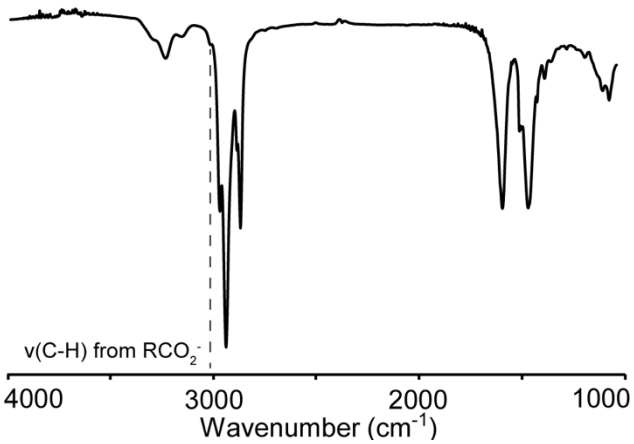


**Figure S6.** FT-IR spectrum of CdSe-$Cd(O_2CR)_2$ in tetrachloroethylene cleaned ten times with a 4.5 M solution of octylamine. The alkenyl C-H stretching frequency at $\nu = 3005$ $cm^{-1}$ is distinctly from unsaturated carboxylate species and not primary amines.

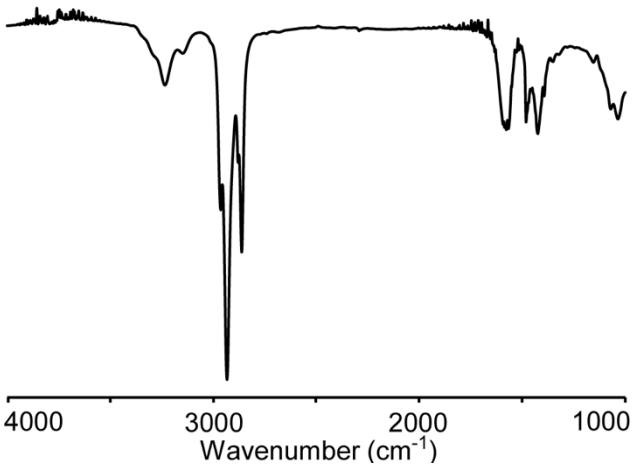


**Figure S7.** FT-IR spectrum of CdSe-$NH_2C_8H_{17}$ in tetrachloroethylene.

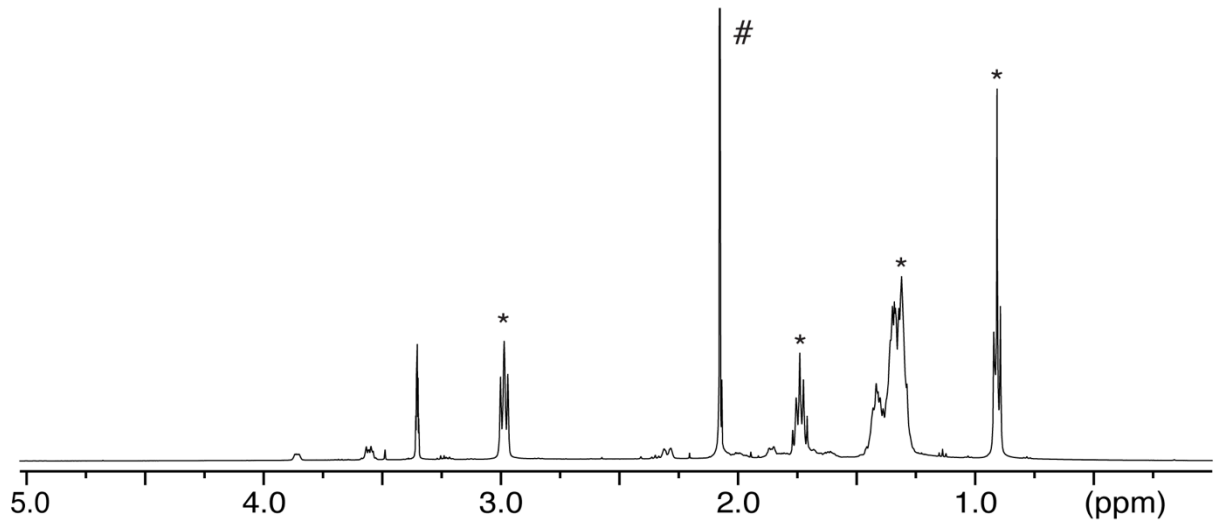


**Figure S8**. $^{1}$H NMR of a CdSe-$NH_2C_8H_{17}$ sample digested in deuterium chloride. The resonances labelled with an asterisk (*) correspond to octylammonium chloride-$d_1$ formed from remaining octylamine after removal of volatiles. In addition, some toluene (labelled #) remained in the sample after removal of volatiles. The excess signal of the methyl resonance that did not correspond to octylammonium species (obtained by comparing the integral of the methyl resonance to the integral of the α-proton resonance at 3.0 ppm) was integrated against an internal standard (pyridine, δ = 8.24 ppm, 2H) to determine the amount of methyl impurities in the nanocrystal sample. This value ranged from 1-3 unknown impurities per nanocrystal.

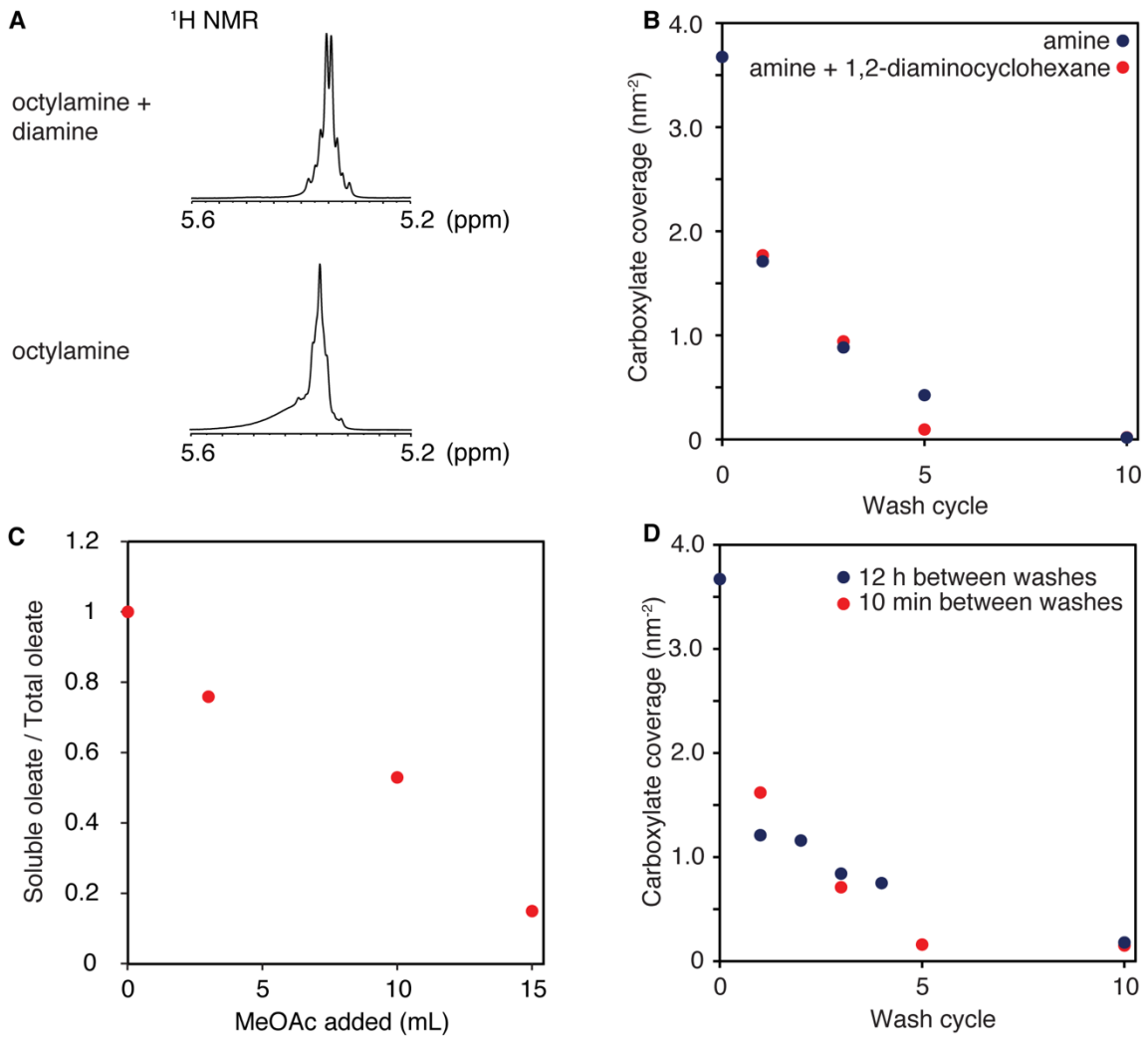


**Figure S9**. (A) Vinyl region of $^{1}$H NMR spectra of CdSe-Cd($O_2$CR)$_2$ in a 4.5 M octylamine solution (bottom) and in a 4.5 M octylamine / 0.5 M 1,2-diaminocyclohexane solution (top). The addition of the diamine aids in removing the cadmium oleate from the surface of the nanocrystal, however the presence of the diamine greatly decreases the solubility of the surface-displaced cadmium carboxylate adduct. (B) Carboxylate coverage as a function of precipitation cycle for a cleaning solution of 4.5 M octylamine in toluene (blue) and a cleaning solution of 4.5 M octylamine / 0.5 M 1,2-diaminocyclohexane in toluene (red). (C) Relative oleate concentrations in the isolated supernatant recovered after centrifugation as a function of methyl acetate added to a solution of CdSe-Cd($O_2$CR)$_2$ and 5 M octylamine / 0.5 M 1,2-diaminocyclohexane in toluene. The

decrease in oleate concentration in the supernatant indicates that cadmium oleate species precipitate simultaneously with the nanocrystals. (D) Carboxylate coverage as a function of precipitation cycles for CdSe-$Cd(O_2CR)_2$ samples allowed to stir for 10 min (red) and 12 hours (blue) in a 4.5 M octylamine / 0.5 M 1,2-diaminocyclohexane toluene solution before precipitation with methyl acetate.

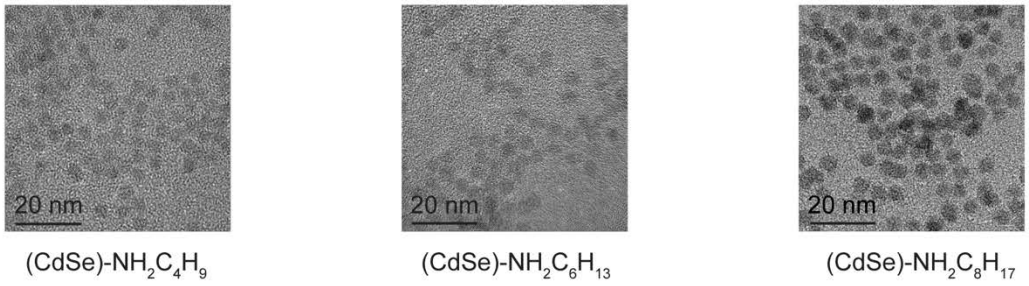


**Figure S10**. Transmission electron micrographs of (CdSe)-$NH_2R$ ($d$ = 5.3 nm) where R = *n*-butyl (left), *n*-hexyl (middle), or *n*-octyl (right). Scale bar is 20 nm.

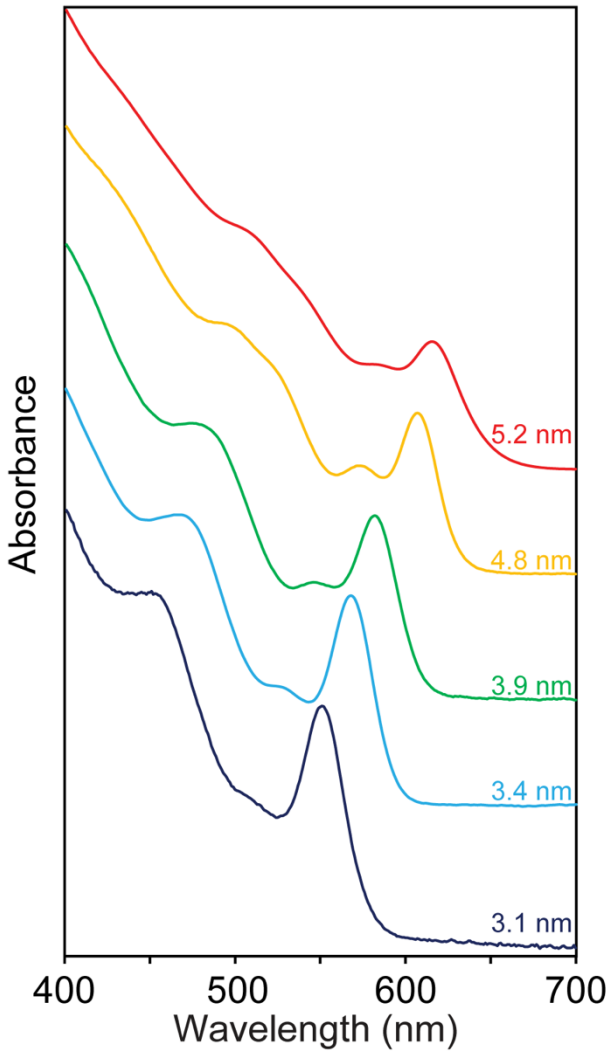


**Figure S11**. UV-Vis spectra of CdSe-$NH_2C_8H_{17}$ of various sizes (d = 3.1, 3.4, 3.9, 4.8, and 5.2 nm).

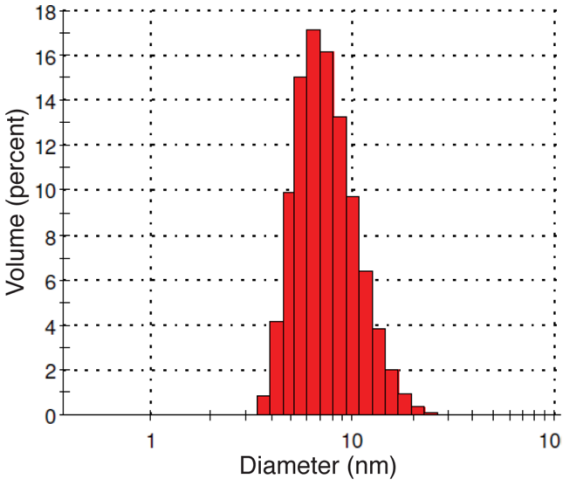


| [amine] (mM) | size (nm) |
|---|---|
| 2.1 | 16.1 |
| 2.5 | 8.1 |
| 13.7 | 8.4 |
| 25.4 | 7.9 |
| 116.4 | 8.7 |

**Figure S12**. (left) Dynamic Light Scattering (DLS) measurements of a CdSe-$NH_2C_8H_{17}$ sample in a 2.5 mM octylamine solution in toluene. (right) Diameters of the species calculated from DLS measurements as a function of amine concentration. For all measurements the concentration of nanocrystals was 50 μM (50 amines per NC). Note: over a period of months these particles aggregated and precipitated at this concentration.

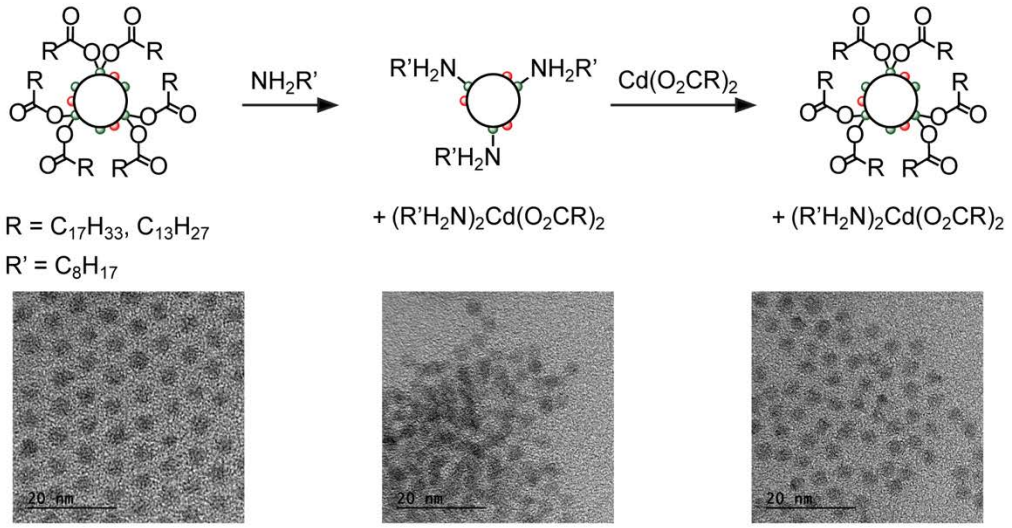


**Figure S13**. (top) Reversible L-Type promoted Z-Type displacement chemistry. (bottom) Transmission electron micrographs of CdSe-$Cd(O_2CR)_2$ (left), CdSe-$NH_2C_8H_{17}$ (right), and CdSe-$Cd(O_2CR)_2$ synthesized from rebinding cadmium oleate to the surface of CdSe-$Cd(O_2CR)_2$. Scale bar is 20 nm ($d$ = 4.2 nm).

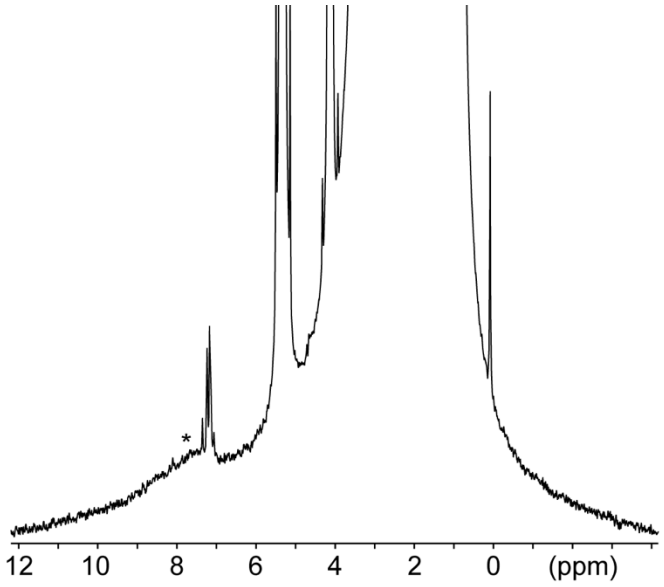


**Figure S14**. $^1$H NMR spectrum of CdSe-$NH_2R'/[O_2CR]^-[H_3NR']^+$ nanocrystals in $CD_2Cl_2$. The sharp resonances around 7.1 ppm are due to residual benzene and toluene. The asterisk (*) denotes the center of a broad resonance tentatively assigned to $[NH_3R']^+$.

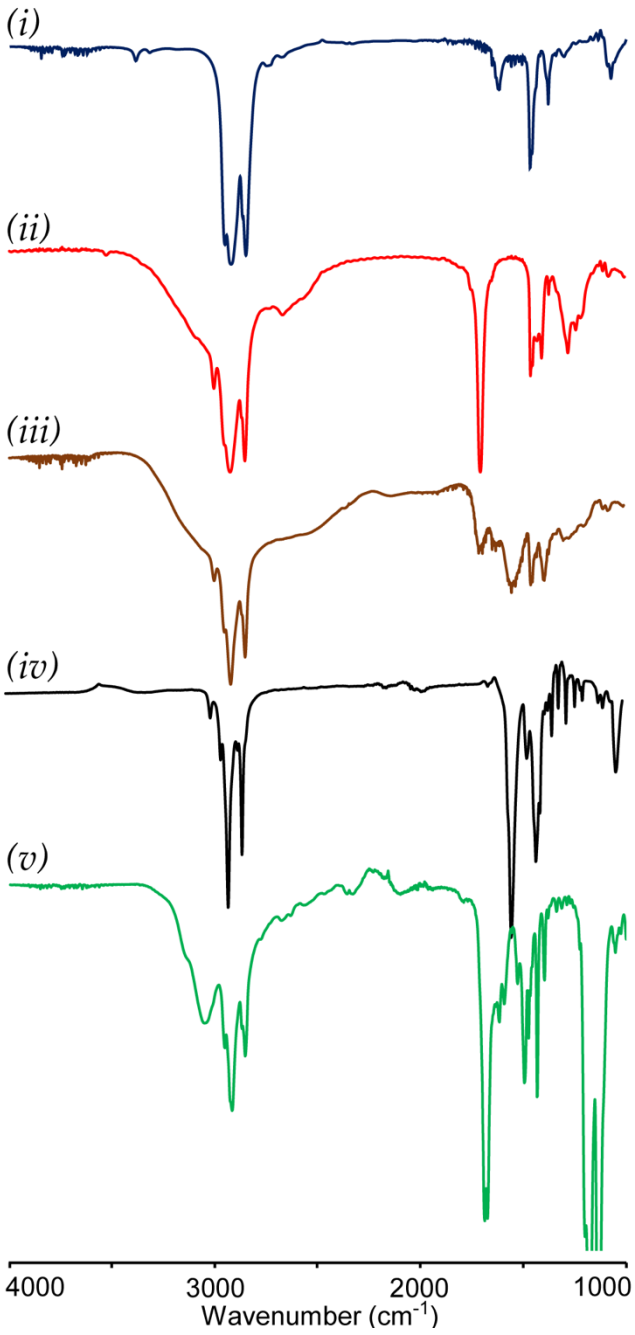


**Figure S15.** FT-IR spectra of *n*-octylamine (*i*), oleic acid (*ii*), 1:1 mixture of *n*-octylamine and oleic acid (*iii*), cadmium oleate (*iv*), and *n*-octylammonium trifluoroacetate (*v*) in tetrachloroethylene.

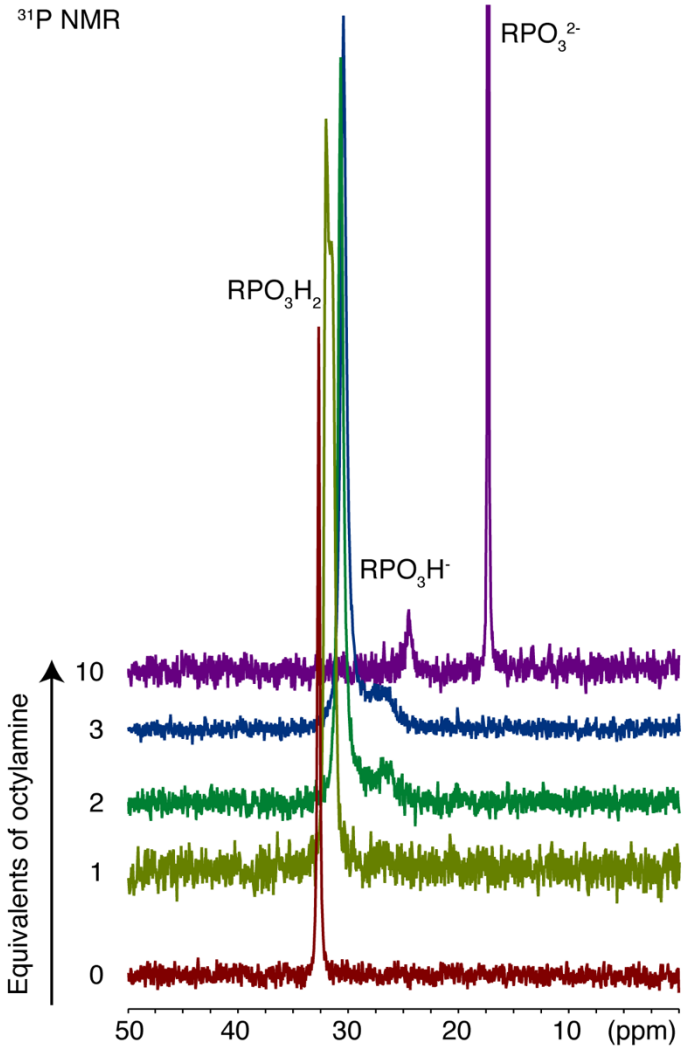


**Figure S16**. $^{31}$P NMR spectra of neat octadecylphosphonic acid (ODPA) in benzene-$d_6$ (red) and 1, 2, 3, and 10 equivalents of *n*-octylamine. The addition of *n*-octylamine deprotonates ODPA (δ = 32 ppm), forming the monohydrogen $RPO_3H^-$ (δ = 27 ppm) and $RPO_3^{2-}$ (δ = 17 ppm) species.

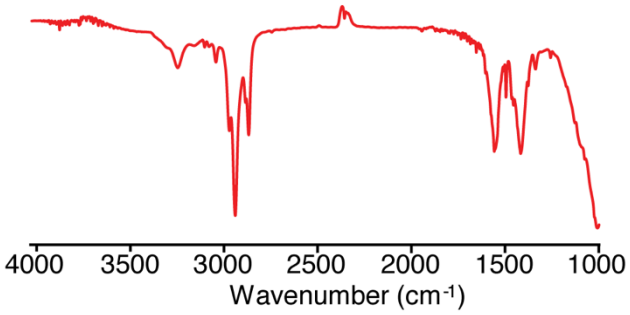


**Figure S17**. FT-IR spectrum of CdSe-$NH_2R'/[O_2C\text{-}NHR]^-[NH_3R]^+$ in tetrachoroethylene.

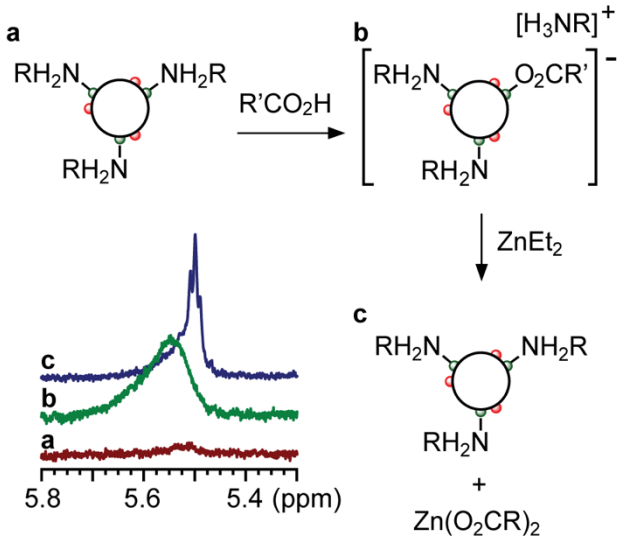


**Figure S18**. Vinyl region of the $^1H$ NMR spectra for CdSe-$NH_2C_8H_{17}$ (a, red), CdSe-$NH_2R'/[O_2CR]^-[NH_3R']^+$ (b, green), and, CdSe-$NH_2R'/[O_2CR]^-[NH_3R']^+$ treated with one equivalent of $ZnEt_2$ (c, blue).

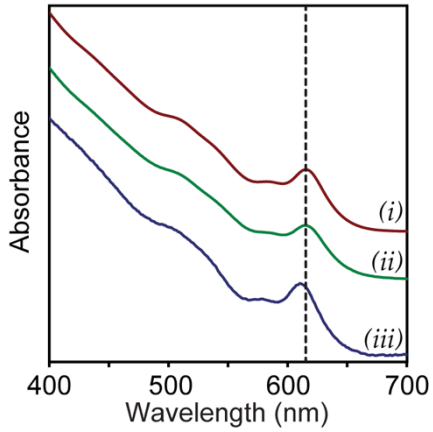


**Figure S19**. UV-Vis spectra of CdSe-$Cd(O_2CR)_2$ (*i*), CdSe-$NH_2C_8H_{17}$ (*ii*), and CdSe-$NH_2C_8H_{17}$/$[O_2CR]^-[NH_3C_8H_{17}]^+$ after addition 0.5 equivalents of diethylzinc (*iii*). The vertical dashed line defines the location of the peak maximum of the first electronic transition in (*i*).

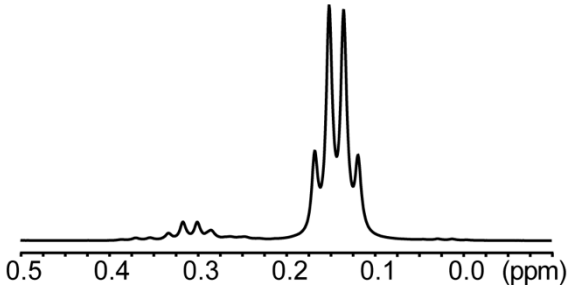


**Figure S20**. $^1$H NMR spectrum of CdSe-$NH_2R'$/$[O_2CR]^-[NH_3R']^+$ treated with one equivalent of $ZnEt_2$. Two peaks are seen in the region between 0.0 and 0.5 ppm. The larger quartet at 0.15 ppm is resonances from the methylene protons in diethylzinc. The smaller resonance at 0.33 ppm indicates the formation of diethylcadmium.

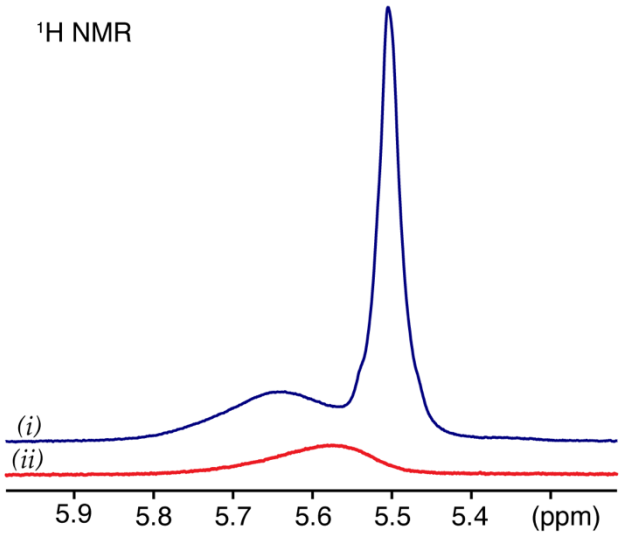


**Figure S21.** Alkene region of the $^{1}$H NMR spectra of CdSe-Cd($O_2$CR)$_2$ treated with oleic acid *in situ* (*i*) and CdSe-Cd($O_2$CR)$_2$/H$O_2$CR obtained after isolation and purification (*ii*). Integration against an internal ferrocene standard ($\delta$ = 4.0 ppm, not shown) yields an oleate surface coverage of 1.14 nm$^{-2}$, roughly twice the coverage of the starting Cd-Cd($O_2$CR)$_2$ nanocrystals (0.59 nm$^{-2}$).

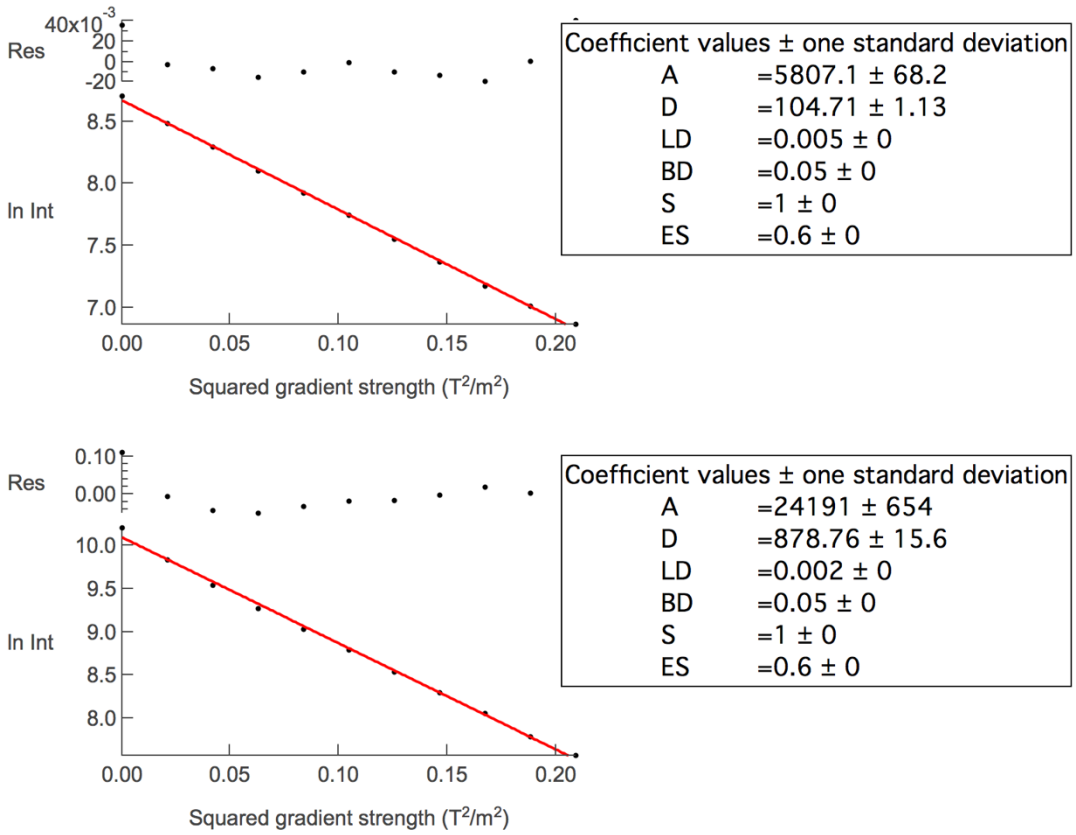


**Figure S22**. Mono-exponential fits of the decay curves of the alkene resonances generated from DOSY spectra of oleic acid bound CdSe-Cd($O_2CR$)$_2$ (top) and oleic acid (bottom) in methylene chloride-$d_2$.

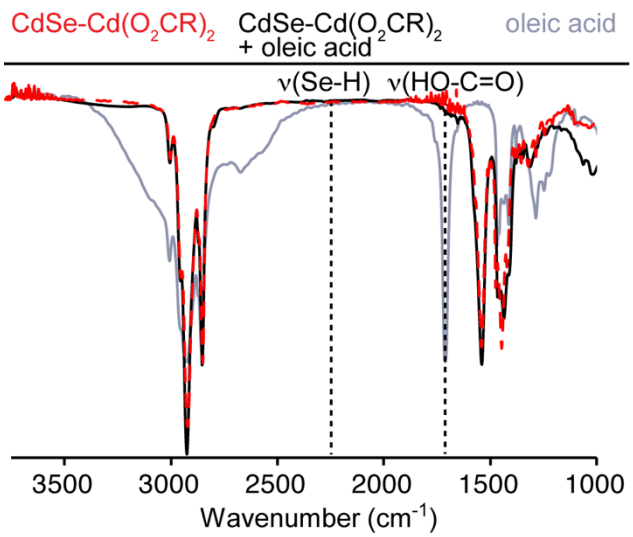


**Figure S23.** FT-IR spectra of CdSe-Cd($O_2CR$)$_2$ (dashed, red), CdSe-Cd($O_2CR$)$_2$/$HO_2CR$ (solid, black), and oleic acid (faded, blue) in tetrachloroethylene. The absence of a selenol stretch around 2300 $cm^{-1}$ and a $CO_2H$ stretch around 1710 $cm^{-1}$ make it difficult to identify the manner in which oleic acid binds to the nanocrystal surface.

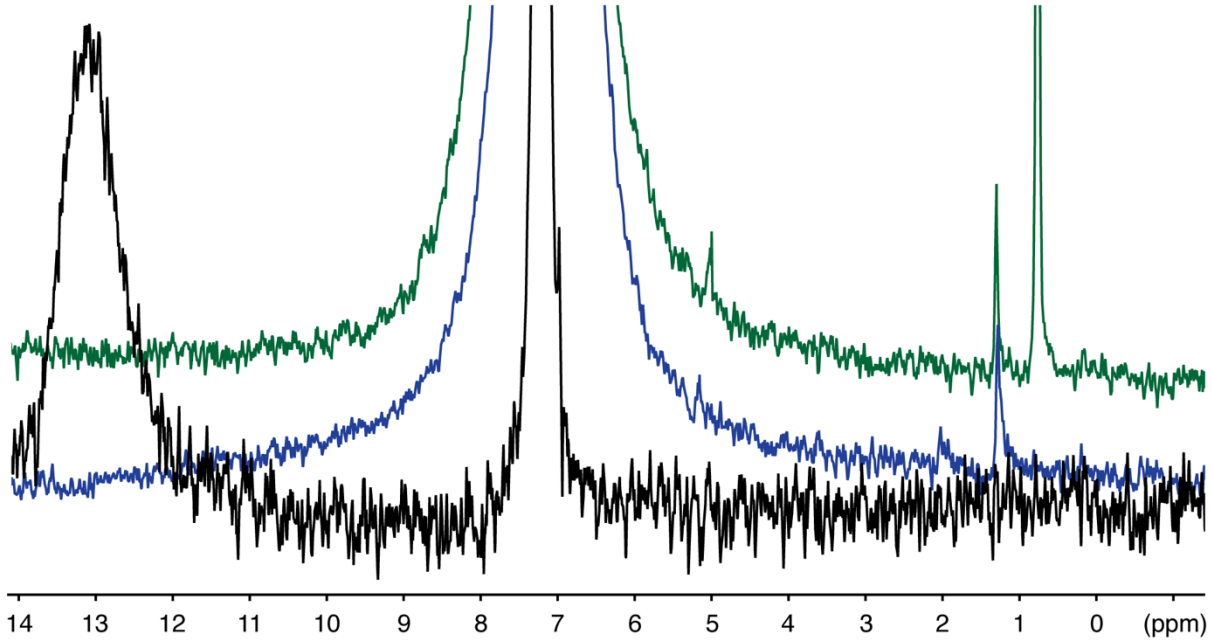


**Figure 24**. $\{^1H\}^2H$ NMR spectra of oleic acid-$d_1$ (bottom), CdSe-$Cd(O_2CR)_2$/$RCO_2D$ (middle), and CdSe-$Cd(O_2CR)_2$/$RCO_2D$ treated with 10 uL of diethylzinc (top). The resonance at 0.8 ppm corresponds to ethane-$d_1$ produced from the deprotonation of oleic acid-$d_1$ by diethylzinc.

| CdSe-L | Ligand concentration (mM) | Nanocrystal diameter (nm) | Ligand surface coverage ($nm^{-2}$) |
|---|---|---|---|
| -$Cd(O_2CR)_2$ | 220 | 3.67 | 1.75 |
| -$Cd(O_2R)_2$<br>-$CH_3$ | 232<br>3.3 | 4.01 | 2.84<br>0.04 |
| -$Cd(O_2CR)_2$<br>-$C_{17}H_{33}CO_2H$ | 10.8<br>9.3 | 3.49 | 0.59<br>0.55 |
| -$NH_2C_8H_{17}$ | 270 | 3.40 | 3.27 |
| -$NH_2C_8H_{17}$<br>-$[NH_3C_8H_{17}]^+[C_{17}H_{33}CO_2]^-$ | 290<br>1.1 | 5.30 | 43.6<br>0.17 |
| -$NH_2C_8H_{17}$<br>$[NH_3C_8H_{17}]^+[NHC_8H_{17}CO_2]^-$ | 42.7<br>2.74 | 5.30 | 2.02<br>0.13 |
| -$NH_2C_8H_{17}$<br>-$[NH_3C_8H_{17}]_n^+[C_{18}H_{37}PO_3H_{2-n}]^-$<br>(n = 1, 2) | 21<br>21 | 5.30 | 2<br>2 |

**Table S1**. Quantitative analysis of nanocrystals and ligands for example nanocrystal samples discussed in the main text.